Raman-excited spin coherences in nitrogen-vacancy color centers in diamond

P. R. Hemmer

Air Force Research Laboratory, Sensors Directorate, Hanscom Air Force Base, Massachusetts 01731

A. V. Turukhin and M. S. Shahriar

Research Laboratory of Electronics, Massachusetts Institute of Technology, 77 Massachusetts Avenue, Cambridge, Massachusetts, 02139

J. A. Musser

Texas A&M University, College Station, Texas 77843

Raman-excited spin coherences were experimentally observed in nitrogen-vacancy (N-V) diamond color centers by means of nondegenerate four-wave mixing and electromagnetically induced transparency. The maximal absorption suppression was found to be 17%, which corresponds to 70% of what is possible given the random geometric orientation of the N-V center in diamond. In the context of quantum computing in solids, this level of transparency represents efficient preparation of quantum bits, as well as the ability to perform arbitrary single-quantum-bit rotations. © 2001 Optical Society of America

OCIS codes: 190.5660, 270.4180, 300.6250, 270.1670.

The use of optical Raman interactions to excite spin coherences in solid materials has numerous potential applications, ranging from low-power nonlinear optics[1] to high-temperature spectral hole burning memories[2,3] to solid-state quantum computing.[4] The interest in Raman excitation lies in the fact that it allows spin coherences to be efficiently excited and manipulated by use of optical laser fields while coupling to the environment, and hence the long spin-coherence lifetimes needed for optical memories and quantum computing, is maintained. Recently proof-of-principle experiments performed in Pr-doped Y_2SiO_5 (Pr:YSO) demonstrated the potential advantage of Raman-excited spin coherences for optical storage.[5] However, Pr:YSO has a weak optical oscillator strength ($\sim 10^{-7}$), as do many other spectral hole burning materials. This weak oscillator strength limits many potential applications because the ability to achieve efficient Raman excitation of spin coherence depends on the product of the oscillator strength and the laser intensity. For memory applications, this small oscillator strength limits the operating temperature. For quantum computing, the small oscillator strength limits the gate speed and hence the number of quantum logic operations that can be performed within the spin-coherence lifetime.[6–8]

For this reason, in the current experiment we chose to use nitrogen-vacancy (N-V) color centers[9] in diamond because they have a large optical oscillator strength (~ 0.1). They also have relatively long spin-coherence lifetimes ($1-100$-μs range) and were previously demonstrated to exhibit Raman heterodyne signals.[10,11] The sample that we used is estimated to have ~ 30 parts in 10^6 N-V color centers and has a peak optical density of ~ 0.6 for a 1-W/cm^2 probe intensity at 15 K, on the zero-phonon line, near 637-nm optical wavelength. Previous work[10] showed that an applied magnetic field of ~ 1 kG along the (111) direction is required for observation of Raman heterodyne signals and therefore is needed for Raman-excited spin coherences. Figure 1 shows an energy-level diagram of the N-V center. The Raman transition frequency (~ 120 MHz) is determined by the spacing between the $S = 0$ and $S = -1$ ground-state spin sublevels. This spacing is controlled by the magnitude of the applied magnetic field. At this field strength, the $S = 0$ and $S = -1$ ground sublevels for (111)-oriented N-V centers are near an anticrossing [Fig. 1(a)]. This gives a partial mixing of the spin sublevels, which enhances the Raman transition strength that otherwise would be small owing to the small spin-orbit coupling.[12]

Laser beams R1 and R2 in Fig. 1(b) act as Raman pump beams to produce a two-photon ground-state coherence via coherent population trapping.[13] Laser beam P acts as a probe beam that is diffracted from a phase grating produced by the two-photon coherence and generates a diffracted beam, D, according to phase-matching conditions $\mathbf{k}_D = \mathbf{k}_{R2} - \mathbf{k}_{R1} + \mathbf{k}_p$. To enhance signal-to-noise ratio, a heterodyne detection scheme is sometimes used to detect beam D. All the laser fields shown are derived from a single dye laser output by use of acousto-optic frequency shifters. This approach greatly relaxes the dye laser frequency-stability requirements, since the resonant Raman interaction is insensitive to correlated laser jitter.

To match the energy-level spacings and laser beam frequencies shown in Fig. 1(b), we downshifted Raman beams R1 and R2, and probe beam P from the original laser frequency by 400, 280, and 420 MHz, respectively. To generate line shapes, we scanned the frequency of beam R2 near the 120-MHz Raman transition frequency with the frequencies of beams R1 and P held fixed. The intersection angle of the Raman beams was $\sim 3.5°$ in the plane of the optical table.
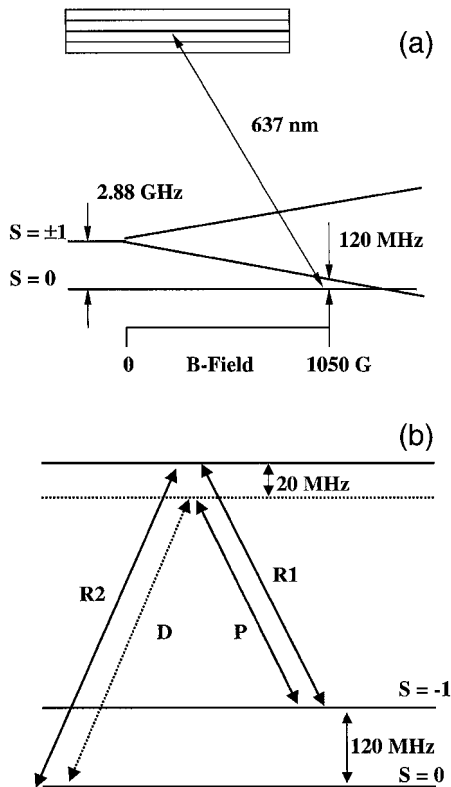
Fig. 1. (a) Energy-level splitting of N-V diamond as a function of magnetic field strength applied in the (111) direction. (b) Λ-shaped three-level system interacting with Raman beams and a probe to generate a NDFWM signal at a magnetic field strength of ~1000 G.

The direction of probe beam P was optimized for diffraction efficiency but was 3.5° out of the plane of the optical table. An additional beam from the argon laser at 514.5 nm was also directed into the sample to serve as a repump. Without this repump beam, the N-V center would exhibit persistent spectral hole burning owing to reorientation of the N-V center in the diamond lattice, and no cw signal would be seen after a short time.[14] In contrast with our previous studies of Pr:YSO, here the repump beam does not provide spectral selectivity for the four-wave mixing signal, and therefore the optical transition is strongly inhomogeneously broadened. All laser beams were linearly polarized and focused into the crystal by a 150-mm focal-length lens, producing a spot with a diameter of ~100 μm. During the experiment, the sample was maintained at a temperature of 15 K inside the Janis helium-flow cryostat. The magnetic field was applied by a pair of Helmholtz coils. A representative nondegenerate four-wave mixing (NDFWM) signal is shown in Fig. 2 as a function of the frequency difference between Raman beams. The line shape was taken at intensities substantially below saturation limits (see below). As shown, the Raman linewidth is ~5.5 MHz, which is comparable to the 5-MHz inhomogeneous width of the spin transition[14] and much smaller than both the homogeneous width of the optical transition (~50 MHz) and the laser jitter (~100 MHz). This suboptical transition linewidth is taken as evidence of the Raman process. The maximal

diffraction efficiency was found to be 0.5% for a very weak probe. This diffraction efficiency is reasonable given the probe detuning and the absorption owing to the high optical density of the sample.

To evaluate the relative matrix elements of our Raman system, we investigated the NDFWM signal amplitude as a function of Raman laser beam intensities. The results are shown in Fig. 3. The saturation intensities were found to be 36 and 56 W/cm² for optical transitions resonant with Raman beams R1 and R2, respectively. The fact that the observed saturation intensities for the Raman-excited spin coherence are much larger than those predicted for a single isolated color center is due to the large inhomogeneous broadening of the optical transition. For the data shown in Fig. 3, the intensity of the probe beam was 1.6 W/cm², which is substantially below its measured saturation intensity (48 W/cm²). The intensity of the repump beam was ~10 W/cm².

Electromagnetically induced transparency[15] (EIT) was also observed in the N-V diamond color center. To do this, we greatly reduced the intensity of Raman beam R2 to 1 W/cm² and used it as a probe, while the other Raman beam (R1) was increased to the maximum available intensity of 280 W/cm² and served as the coupling beam. The NDFWM probe beam (P) was blocked during the experiment. The representative experimental trace of the transmission of the probe
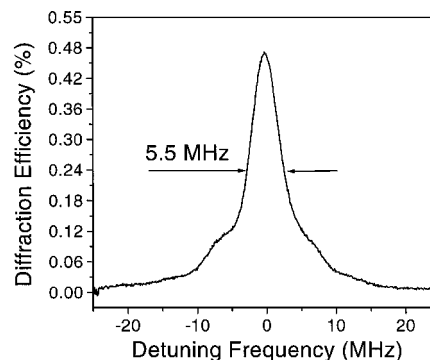

Fig. 2. NDFWM signal efficiency at 15 K. The intensities of R1, R2, P, and the repump beam were 1.2, 1.6, 5.6, and 10 W/cm², respectively. The central difference frequency was 120 MHz.
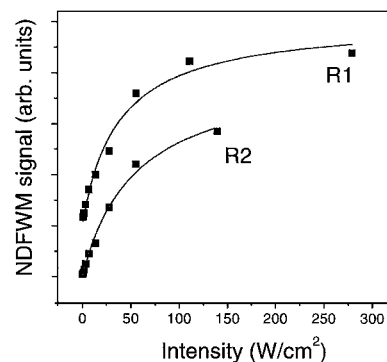

Fig. 3. Saturation curves for beams R1 and R2 (the plots are vertically shifted for clarity). The intensity of the probe was 1.6 W/cm². The intensity of the complimentary Raman beam was ~1.5 W/cm² for both curves. The temperature of the sample was 15 K.
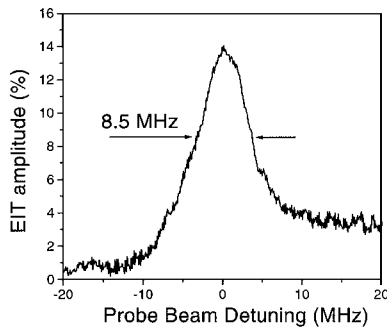
Fig. 4. EIT amplitude relative to the peak probe absorption versus probe detuning in N-V diamond at 15 K for a coupling field intensity of 280 W/cm^2. The intensities of the probe and the repump were 1 and 10 W/cm^2, respectively. The sloping background is due to the frequency-dependent efficiency of the acousto-optic shifter.

as a function of Raman detuning are presented in Fig. 4. The maximal value of transparency is 17% of the background absorption (optical density, 0.3). The background absorption is reduced in the presence of the pump beam owing to off-resonant pump-induced persistent spectral hole burning. We point out that the observed value of transparency is large for such strong inhomogeneous optical broadening. This result is in good agreement with a simplified theoretical model that takes into account the inhomogeneous broadening and the fact that only one in four color centers has the correct orientation relative to the magnetic field. Fitting the experimental EIT spectrum to the model gives a rms Rabi frequency of ~160 MHz. For applications in which single atoms are excited, the theoretical model shows that resonant atoms with the correct orientation, when driven by such a large Rabi frequency, would exhibit close to 100% transparency. Finally, the observed EIT linewidth of 8.5 MHz is substantially smaller than the laser jitter and the optical homogeneous linewidth and is even smaller than the 24-MHz radiative contribution to the optical linewidth. The fact that the width of the EIT peak exceeds the inhomogeneous linewidth of the ground-state spin transition is most likely due to power broadening, since a relatively high laser intensity was needed to produce efficient EIT in the presence of the large optical inhomogeneous broadening.

In summary, we have observed electromagnetically induced transparency and nondegenerate four-wave mixing generation in an inhomogeneously broadened optically thick crystal of N-V diamond. The observed maximal value of EIT of 17%, which corresponds to 70% of what is possible (i.e., 25%) given the random geometric orientation of the N-V center in diamond, makes it possible to use this material in a variety of EIT applications, such as nonlinear image processing,[16] optical data storage in solids, and solid-state quantum computing. In particular, for quantum computing applications, we estimate that this particular N-V diamond crystal should be capable of more than 500 operations. This estimation is based on the fitted 160-MHz Rabi frequency and the observed spin Rabi-flop decay time of 1 μs. However, the Rabi-flop decay rate is dominated by inhomogeneous broadening, and the actual spin-coherence lifetime is expected to be ~40 μs, based on published spin-echo decay measurements,[17] so many more operations should be possible.

References

1. M. D. Lukin, P. R. Hemmer, M. Loffler, and M. O. Scully, Phys. Rev. Lett. **81,** 2675 (1998).
2. H. Lin, T. Wang, and T. W. Mossberg, Opt. Lett. **20,** 1658 (1995).
3. X. A. Shen, E. Chiang, and R. Kachru, Opt. Lett. **19,** 1246 (1994).
4. C. Williams and S. Clearwater, *Explorations in Quantum Computing* (Springer-Verlag, New York, 1998).
5. B. S. Ham, M. S. Shahriar, M. K. Kim, and P. R. Hemmer, Opt. Lett. **22,** 1849 (1997).
6. M. S. Shahriar, P. R. Hemmer, S. Lloyd, J. A. Bowers, and A. E. Craig, "Solid state quantum computing using spectral holes," http://xxx.lanl.gov/pdf/quant-ph0007074.
7. M. D. Lukin and P. R. Hemmer, Phys. Rev. Lett. **84,** 2818 (2000).
8. T. Pellizzari, S. A. Gardiner, J. I. Cirac, and P. Zoller, Phys. Rev. Lett. **75,** 3788 (1995).
9. A. Lenef, S. W. Brown, D. A. Redman, S. C. Rand, J. Shigley, and E. Fritsch, Phys. Rev. B **53,** 13427 (1996).
10. X. F. He, N. B. Manson, and P. T. H. Fisk, Phys. Rev. B **47,** 8809 (1993).
11. N. B. Manson, X. F. He, and P. T. Fisk, J. Lumin. **53,** 49 (1992).
12. J. P. O. Martin, J. Lumin. **81,** 237 (1999).
13. H. R. Gray, R. M. Whitley, and C. R. Stroud, Opt. Lett. **3,** 131 (1990).
14. N. Manson, Laser Physics Centre, Australian National University, Canberra 0200, Australia (personal communication, June 2000).
15. S. E. Harris, Phys. Today **50**(7), 36 (1997) and references therein.
16. X. A. Chen and R. Kachru, Opt. Lett. **17,** 520 (1992).
17. E. van Oort, N. B. Manson, and M. Glasbeek, J. Phys. C **21,** 4385 (1988).